Acta Crystallographica Section B
Structural Science
ISSN 0108-7681

Packing modes of (*R*,*R*)-tartaric acid esters and amides

Urszula Rychlewska* and Beata Warżajtis

Department of Crystallography, Faculty of Chemistry, Adam Mickiewicz University, Grunwaldzka 6, 60-780 Poznań, Poland

Correspondence e-mail: urszula@krystal.amu.edu.pl

Received 22 November 1999
Accepted 16 March 2000

The molecular packing modes of a series of mono- and diamides of (*R*,*R*)-tartaric acid are discussed on the basis of their crystal structures. Derivatives include combinations of methylester, amide, *N*-methylamide and *N*,*N*-dimethylamide groups, both symmetrically and asymmetrically substituted. The symmetrically substituted derivatives do not utilize their C_2 symmetry in the crystal. The packing of primary tartramides seems to be driven by NH···O=C hydrogen bonds and supplemented by strong OH···O=C and weak NH···OH bonds. On the other hand, in derivatives containing methylester and/or methylamide groups OH···OH···O=C hydrogen-bond patterns seem to dominate. Types of aggregates, characteristic for the investigated derivatives, include cyclic dimers and ring systems analogous to the dimers, but formed by two different although complementary functional groups, as well as sets of chains aligned in a manner resembling the helical arrangement of peptides. The helices are formed along the screw axis with an identity period of approximately 5 Å. In tartramic acids, containing in one molecule both carboxyl and amide functions, in competition between the two groups to control the molecular arrangement, the latter dominates, unless it is *N*-substituted tartramide, in which case the carboxyl group predominates. Problems with packing, which occur in some of the structures owing to the steric bulk of the methyl groups, are overcome by changes in conformation (esters) or by co-crystallization with solvent water molecules (methylamides and dimethylamides). These derivatives are also more likely to crystallize with multiple asymmetric units.

1. Introduction

The mode of molecular aggregation in terms of characteristic hydrogen-bond motifs formed by common functional groups is of increasing interest in many fields of science (Aakeröy, 1997; Brock & Dunitz, 1994; Desiraju, 1989; Gavezzotti, 1994). While packing preferences of some of the most common functional groups such as hydroxyl, carboxyl or amide have already been well established (Berkovitch-Yellin & Leiserowitz, 1982; Berkovitch-Yellin *et al.*, 1983; Brock & Duncan, 1994; Etter, 1990; Leiserowitz, 1976; Leiserowitz & Hagler, 1983; Leiserowitz & Tuval, 1978; Leiserowitz & Schmidt, 1969; Weinstein & Leiserowitz, 1980), data concerning the packing preferences of amide, carboxyl or ester groups accompanied by a hydroxyl group in the α-position are rather scarce.

In this paper we present an analysis of the most common packing modes observed in the crystal structures of (*R*,*R*)-

Table 1
The structures discussed.

Abbreviations: numbers 1, 2 and 3 designate primary, secondary and tertiary amide substituents, respectively, while OH and OM represent hydroxyl and methyl ester substituents, respectively.

	X	*Y*	Abbreviation
(*R*,*R*)-(+)-Tartaric acid monoamide	OH	NH_2	HOH1
(*R*,*R*)-(+)-Tartaric acid mono(*N*-methylamide) monohydrate	OH	NHMe	HOH2
(*R*,*R*)-(+)-Tartaric acid diamide	NH_2	NH_2	HN11
(*R*,*R*)-(+)-Tartaric acid *N*-methyldiamide	NH_2	NHMe	HN12
(*R*,*R*)-(+)-Tartaric acid *N*,*N*-dimethyldiamide monohydrate	NH_2	NMe_2	HN13
(*R*,*R*)-(+)-Tartaric acid *N*,*N*′-dimethyldiamide monohydrate	NHMe	NHMe	HN22
Dimethyl (*R*,*R*)-(+)-tartrate	OMe	OMe	HOM
(*R*,*R*)-(+)-Tartaric acid monoamide monomethylester	OMe	NH_2	HOM1
(*R*,*R*)-(+)-Tartaric acid mono(*N*,*N*-dimethylamide) monomethyl ester	OMe	NMe_2	HOM3

tartaric acid derivatives. The compounds analysed are the covalent derivatives of (*R*,*R*)-tartaric acid (Table 1). Modifications include the replacement of one or both carboxyl groups by methyl ester, amide, *N*-methylamide and *N*,*N*-dimethylamide functions. Consequently, the systems studied include both symmetrically and asymmetrically substituted derivatives. The paper reports two newly determined crystal structures, namely (*R*,*R*)-tartaric acid monoamide [4-amido-(2*R*,3*R*)-2,3-dihydroxybutanoic acid, HOH1] and (*R*,*R*)-tartaric acid *N*-methyldiamide [*N*-methyl-1,4-(2*R*,3*R*)-(2,3-dihydroxybutanedicarboxamide), HN12], and low-temperature X-ray diffraction results for (*R*,*R*)-tartaric acid *N*,*N*′-dimethyldiamide [*N*,*N*′-dimethyl-1,4-(2*R*,3*R*)-(2,3-dihydroxybutanedicarboxamide), HN22]. The other crystal structures discussed in the paper (HOH2, HN11, HN13, HOM, HOM1, HOM3) have already been published (Gawroński *et al.*, 1997; Rychlewska *et al.*, 1997; Rychlewska *et al.*, 1999; Szarecka *et al.*, 1996), but discussion of their structure has been largely limited to factors responsible for their conformational preferences. The investigated molecules are relatively small, homochiral and contain various common functional groups in the α-position to each other, which leads to many variations in packing. The presence of water molecules in some of the crystal structures is a source of additional complexity. Self-association of tartramides is particularly interesting in view of the fact that the optical rotation of tartrates is strongly dependent on the solvent used: the $[\alpha]_D$ value undergoes a change from positive in polar solvents to negative in chloroform solution and this change in the sign of rotation is explained by the association phenomena of tartrates in nonpolar solvents (Gawroński & Gawrońska, 1999). It is expected that the self-association of tartrates and tartramides in a nonpolar solvent will follow a similar pattern to the association in nonhydrated crystals, while hydrated crystals will mimic the aqueous solvent environment.

The following features can be considered as characteristic for the studied system.

(i) Tartaric acid as a dicarboxylic acid can be converted to its derivatives (esters and amides) by symmetrical or unsymmetrical substitution. We have studied both cases.

(ii) In the closest proximity to the carboxylic (or ester or amide) function a secondary hydroxyl group exists which might be expected to compete for hydrogen bonding with the former groups.

(iii) The investigated derivatives of tartaric acid are homochiral and therefore the packing motifs present in their crystal structures can be formed only between molecules which are either related by proper rotation or by translation, or between molecules from multiple asymmetric units.

(iv) As far as hydrogen-bond donor/acceptor properties of the functional groups are concerned, the majority appear to be both self-complementary and complementary to one another. Therefore, one might expect various types of ring associations *via* the same or different hydrogen-bonding groups.

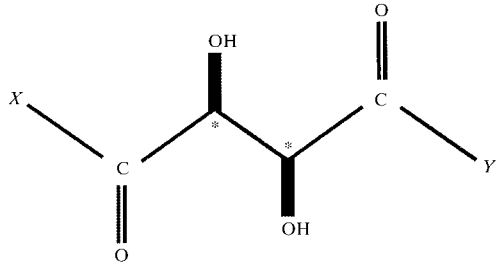

2. Experimental

2.1. Synthesis

The compounds investigated have been obtained in the Laboratory of Natural Products, Department of Chemistry, Adam Mickiewicz University, Poznań, Poland (Gawroński *et al.*, 1997).

2.2. X-ray crystallography

The X-ray data for HOH1, HN12 and HN22, measured on a KUMA KM-4 diffractometer, are summarized in Table 2.[1] The structures were solved by direct methods and refined by full-matrix least-squares procedures. All non-H atoms were refined anisotropically. The hydroxyl H atoms were in difference-Fourier maps and refined isotropically. Methyl H atoms were treated as follows: one methyl hydrogen was located from a difference-Fourier map and the positions of the remaining two were calculated assuming sp^3 hybridization. H atoms bonded to the chiral centers at C2 and C3, and to N atoms were placed in calculated positions. During the refinement all these H atoms were constrained with a riding model and were assigned an isotropic displacement parameter 20% higher than the equivalent isotropic value for the parent atom.

[1] Supplementary data for this paper are available from the IUCr electronic archives (Reference: CF0011). Services for accessing these data are described at the back of the journal.

Table 2
Experimental details.

Computer programs used: data collection: *KM*-4 (Kuma Diffraction, 1991); cell refinement: *KM*-4; data reduction: *DATAPROC* (Gałdecki *et al.*, 1995); structure solution: *SHELXS*86 (Sheldrick, 1990); structure refinement: *SHELXL*93 (Sheldrick, 1993); preparation of material for publication: *SHELXL*93 (Sheldrick, 1993).

	HOH1	HN12	HN22
Crystal data			
Chemical formula	$C_4H_7NO_5$	$C_5H_{10}N_2O_4$	$C_6H_{14}N_2O_5$
Chemical formula weight	149.11	162.15	194.19
Cell setting	Orthorhombic	Tetragonal	Orthorhombic
Space group	$P2_12_12_1$	$P4_12_12$	$P2_12_12_1$
a (Å)	5.9556 (5)	10.594 (1)	5.094 (1)
b (Å)	8.0972 (5)	10.594 (1)	11.243 (2)
c (Å)	11.8960 (8)	13.771 (3)	16.295 (4)
V (Å^3)	573.67 (7)	1545.6 (4)	933.2 (3)
Z	4	8	4
D_x (Mg m^{-3})	1.726	1.394	1.382
Radiation type	Mo $K\alpha$	Mo $K\alpha$	Mo $K\alpha$
Wavelength (Å)	0.71073	0.71073	0.71073
No. of reflections for cell parameters	46	47	40
θ range (°)	12.2–15.0	6.1–12.0	5.9–19.1
μ (mm^{-1})	0.162	0.121	0.120
Temperature (K)	293 (2)	293 (2)	100 (2)
Crystal form	Square pyramid	Tetragonal bipyramid	Needle
Crystal size (mm)	0.5 × 0.5 × 0.5	0.45 × 0.44 × 0.41	0.3 × 0.3 × 0.2
Crystal colour	Colourless	Colourless	Colourless
Data collection			
Diffractometer	KM-4 four circle	KM-4 four circle	KM-4 four circle
Monochromator	Graphite	Graphite	Graphite
Data collection method	θ–2θ scans	θ–2θ scans	θ–2θ scans
Absorption correction	None	None	None
No. of measured reflections	1688	1939	2216
No. of independent reflections	1534	1698	2058
No. of observed reflections	1476	1408	1696
Criterion for observed reflections	$I > \sigma(I)$	$I > \sigma(I)$	$I > \sigma(I)$
R_{int}	0.0109	0.0134	0.1030
θ_{max} (°)	29.06	27.06	27.06
Range of h, k, l	$-8 \rightarrow h \rightarrow 8$ $0 \rightarrow k \rightarrow 11$ $0 \rightarrow l \rightarrow 16$	$0 \rightarrow h \rightarrow 13$ $0 \rightarrow k \rightarrow 13$ $0 \rightarrow l \rightarrow 17$	$-6 \rightarrow h \rightarrow 6$ $0 \rightarrow k \rightarrow 14$ $0 \rightarrow l \rightarrow 20$
No. of standard reflections	2	2	3
Frequency of standard reflections	Every 100 reflections	Every 100 reflections	Every 100 reflections
Intensity decay (%)	0.96	0.89	0.51
Refinement			
Refinement on	F^2	F^2	F^2
$R[F^2 > 2\sigma(F^2)]$	0.0328	0.0415	0.0571
$wR(F^2)$	0.0845	0.1121	0.1460
S	1.020	1.118	1.041
No. of reflections used in refinement	1531	1698	2057
No. of parameters used	103	113	134
H-atom treatment	Riding model	Riding model	Riding model
Weighting scheme	$w = 1/[\sigma^2(F_o^2) + (0.0485P)^2 + 0.1655P]$, where $P = (F_o^2 + 2F_c^2)/3$	$w = 1/[\sigma^2(F_o^2) + (0.0699P)^2 + 0.2727P]$, where $P = (F_o^2 + 2F_c^2)/3$	$w = 1/[\sigma^2(F_o^2) + (0.1129P)^2 + 0.4981P]$, where $P = (F_o^2 + 2F_c^2)/3$
$(\Delta/\sigma)_{max}$	−0.054	0.000	0.000
$\Delta\rho_{max}$ (e Å^{-3})	0.393	0.283	0.276
$\Delta\rho_{min}$ (e Å^{-3})	−0.177	−0.233	−0.263
Extinction method	None	*SHELXL*93 (Sheldrick, 1993)	None
Extinction coefficient	–	0.030 (5)	–

For HN12, the methyl group is disordered (occupancies 60:40; isotropic displacement parameter for the lower occupancy site, methyl H atoms located only for the major conformer). The absolute structure of the crystals was assumed from the known absolute configuration of (*R*,*R*)-tartaric acid. Siemens (1989) Stereochemical Workstation was used to prepare drawings.

3. Discussion

3.1. Conformational preferences of (*R*,*R*)-tartaric acid esters and amides

The conformational preferences for the reported group of compounds have been well established in an isolated state

Table 3
Selected torsion angles (°).

Compound	Conformation	C1—C2—C3—C4	HO—C*—C═O
HOH1	T*sa*	−175.5 (1)	−1.9 (2)
			180.0 (1)
HOH2	T*sa*	173.9 (1)	−15.7 (2)
			176.3 (1)
HN11	T*aa*	−167.0 (2)	−178.2 (2)
			−179.4 (2)
HN12	T*aa*	−179.4 (2)	−176.8 (2)
			−175.5 (2)
HN13	T*as*	178.2 (1)	−165.6 (2)
			21.6 (2)
HN22	T*aa*	171.6 (2)	−179.3 (3)
			172.3 (2)
HOM	T*as*	−169.2 (1)	−176.8 (2)
			0.2 (2)
HOM1 molecule I	T*sa*	171.8 (2)	−3.6 (3)
			178.6 (3)
Molecule II	T*aa*	−175.1 (2)	−176.9 (2)
			167.0 (2)
HOM3 molecule I	T*ss*	163.9 (3)	12.5 (5)
			6.5 (4)
Molecule II	T*ss*	156.2 (3)	12.8 (5)
			8.3 (5)

(Polavarapu *et al.*, 1987), polar and nonpolar solvents and in the solid state (Gawroński *et al.,* 1989, 1997; Hoffmann *et al.*, 1999; Kroon, 1982; Szczepańska & Rychlewska, 1994). Almost invariably, the molecules adopt a planar *T* conformation of the four carbon chain and a planar or nearly planar α-hydroxyacid, ester or amide group (Fig. 1). The C═O/C(α)—O bond system tends to be either *synplanar*, *s*, or *antiplanar*, *a*. While the α-hydroxyacid or α-hydroxyamide groups have strict conformational preferences (*s* for the acid and tertiary amide, and *a* for the primary and secondary amide), the α-hydroxyester group easily adjusts to packing requirements and adopts both *s* and *a* conformations in the crystal (Rychlewska *et al.*, 1997; Szarecka *et al.*, 1996). The T conformation of the four-atom carbon chain is stabilized by intramolecular hydrogen bonds, described by the pattern designator *S*(5) (for a description of pattern designators see, for example, Bernstein *et al.*, 1995, and references therein), and the electrostatic CO/C(β)H and CN/C(β)H coplanar bond interactions. There are quite a few reported exceptions, for which the four-atom carbon chain is bent, namely (*R*,*R*)-*N*,*N*,*N*′,*N*′-tetramethyltartramide and its dibenzoyl derivative (Gawroński *et al.*, 1989; Rychlewska, 1992), (*R*,*R*)-*N*,*N*,*N*′,*N*′-tetracyclohexyldimethoxysuccinamide (*S*)-2,2′-dihydroxy-1,1′-binaphthyl clathrate (Toda *et al.*, 1988), some of the dialkyl tartrate ligands for titanium catalysts for Sharpless asymmetric epoxidation (Pedersen *et al.*, 1987), *O*,*O*′-dibenzoyl-(*R*,*R*)-hydrogen tartrate anion (Hommeltoft *et al.*, 1986) and the monoester of *O*,*O*′-diacetyl-(*R*,*R*)-tartaric acid with (*S*)-timolol (Kivikoski *et al.*, 1993). *Gauche* conformation of the four-atom carbon chain has also been observed in a series of racemic 2,3-disubstituted tartramides (Yamashita *et al.*, 1996).

In the crystal structures discussed in this paper all derivatives adopt the T conformation, with planar or nearly planar α-hydroxyacid, ester or amide groups. Table 3 lists the pertinent torsion angles for all the derivatives in question. Fig. 2 illustrates the molecular structure and labelling scheme for these derivatives for which the new crystal structures are reported in this paper (HOH1, HN12 and HN22). The molecules adopt the T*sa,* T*aa* and T*aa* conformations, respectively. The conformational flexibility of tartrates and the rigidity of

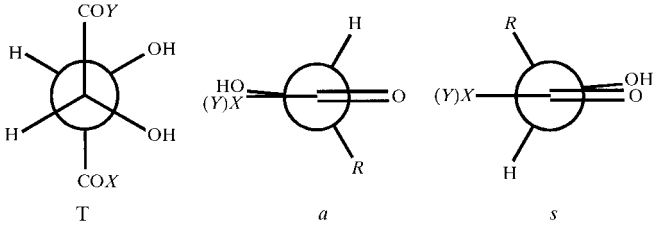

Figure 1
Conformational rotamers characteristic for the presented series of (*R*,*R*)-tartaric acid derivatives. T represents the *trans* orientation of four C atoms constituting the chain, while *s* and *a* describe *synplanar* and *antiplanar* orientations of the hydroxyl substituent with respect to the nearest carbonyl group.

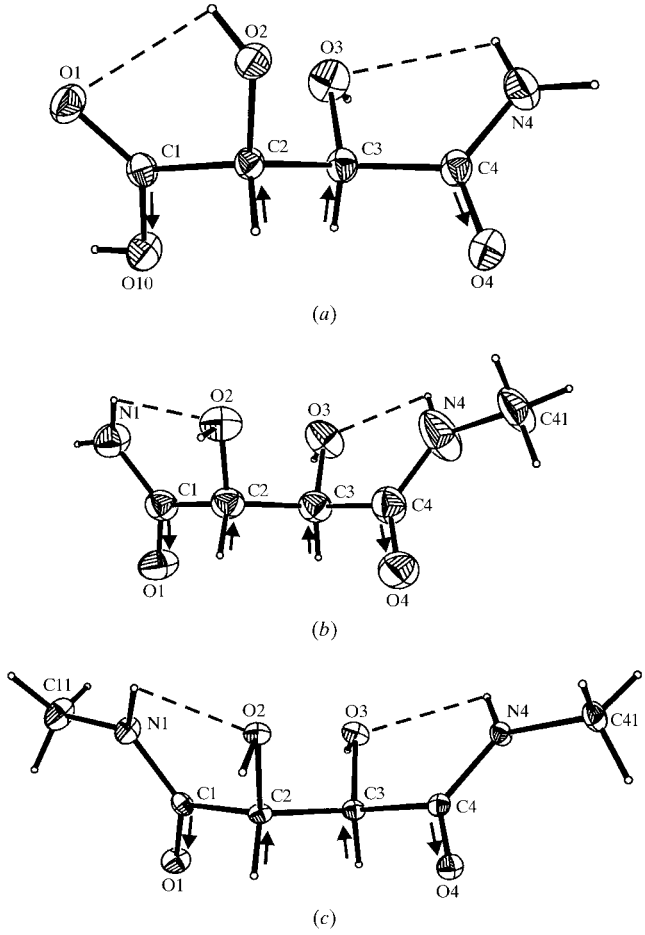

Figure 2
Illustration of the conformations of the newly investigated molecules with atom numbering scheme. (*a*) HOH1, T(*s*,*a*), (*b*) HN12, T(*a*,*a*) (major conformer) and (*c*) HN22, T(*a*,*a*). Thermal ellipsoids are drawn at the 40% probability level. The molecular conformation is stabilized by intramolecular hydrogen bonds (dashed lines) and attractive dipole–dipole interactions (dipoles marked with arrows).

tartramides is reflected in their packing mode, as will be demonstrated below.

3.2. Hydrogen bonds in (*R*,*R*)-tartramides

Hydrogen-bond parameters are listed in Table 4. The major hydrogen-bonding donor groups are N—H in amide, and *N*-methylamide and OH in hydroxyl and carboxylic groups or water molecules. The major hydrogen-bonding acceptor groups are >C═O groups of amide, ester and carboxyl residues, and OH groups either from the parent compounds or from water molecules. The majority of these groups display dual hydrogen-bond functionality and therefore can give rise to hydrogen-bond cooperativity (Jeffrey & Saenger, 1991).

3.2.1. Typical amide···amide hydrogen-bond motifs found in the crystal structures of monoamides and diamides of (*R*,*R*)-tartaric acid. Considering the fact that the majority of the compounds studied contain primary and secondary amide groups, it is not surprising to find that the motifs characteristic for the amide hydrogen bonds (Bernstein *et al.*, 1994; Leiserowitz & Tuval, 1978; Leiserowitz & Schmidt, 1969; Weinstein & Leiserowitz, 1980) are preserved in their crystal structures. However, it should be stressed that these motifs are usually accompanied by additional hydrogen bonds in which hydroxyl groups are involved. Representatives of such patterns are shown in Figs. 3 and 4.

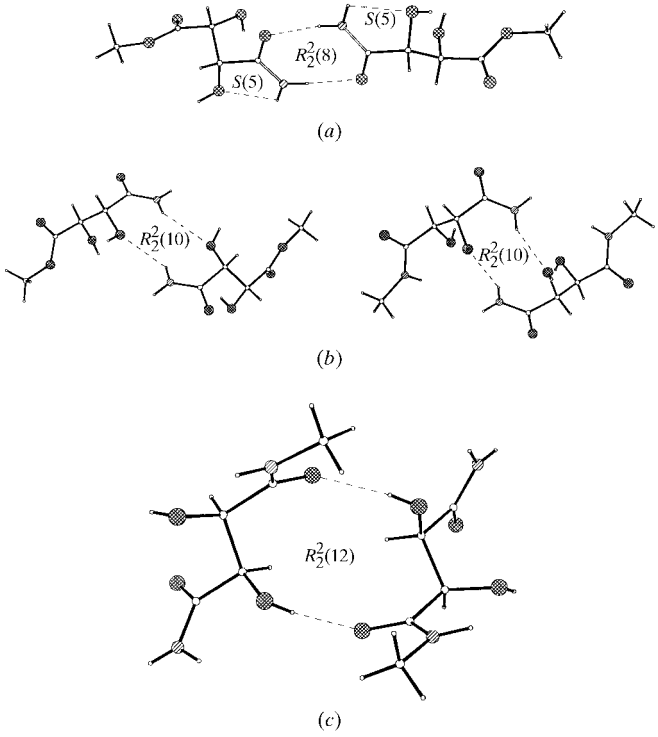

Figure 3
Dimers formed by hydroxyamide groups: (*a*) typical amide dimer [pattern designator $R_2^2(8)$] with N—H_{cis} as a donor to the carbonyl oxygen, accompanied by two *S*(5) motifs (HOM1); (*b*) α-hydroxyamide dimer [pattern designator $R_2^2(10)$] with N—H_{trans} as a donor to the proximal hydroxyl (HOM1, left and HN12, right). Note the close topological similarity of the two molecules and of the dimer formed; (*c*) β-hydroxycarbonyl dimer [pattern designator $R_2^2(12)$] with the distal OH group as a donor to the amide carbonyl oxygen (HN12).

H atoms which are *cis* to the amide carbonyl oxygen form either cyclic dimers R_2^2 (8), as in HOM1 (Fig. 3*a*), where they join two independent molecules, or infinite *C*(4) chains connecting molecules related by a screw axis as observed, for example, in HN12 (Fig. 4*b*) and HN11 (Fig. 11*b*). On the other hand, H atoms which are *trans* to the amide carbonyl oxygen form *C*(4) chains which involve molecules related by a 5 Å translation, as observed in symmetrical diamides of (*R*,*R*)-tartaric acid, HN11 and HN22 (Figs. 4*a*, 11*a* and 10*a*, respectively). The only infinite amide chain around a screw axis that involves *trans* H atoms is observed in the crystal structure of HN13 (Table 4). Besides the motifs characteristic of primary and secondary monoamides, patterns characteristic of diamides can be expected to occur. Of these, the most characteristic for the system studied are the *C*(7) amide chains (see Figs. 5*a* and 10*b*), joining molecules related by a screw axis in a head-to-tail fashion. The motifs are observed in all diamides of (*R*,*R*)-tartaric acid that contain a combination of primary and/or secondary amide groups (HN11, HN12 and HN22). Moreover, an analogous *C*(7) chain appears in the crystal structure of tartaric acid monoamide (HOH1). It involves a primary amide group as a donor and a carboxylic carbonyl group as an acceptor (Fig. 5*b*). This might be considered as one of the many examples of a carboxyl or α-hydroxycarboxyl group mimicking the role of an amide group in hydrogen-bond formation, an observation well known in the field of co-crystal formation (Wash *et al.*, 1997, and references therein). One more example of such behaviour can be found in the crystal structure of HOH1, as will be demonstrated below. Quite surprisingly, no bond of NH···O═C type is formed to the ester carbonyl group.

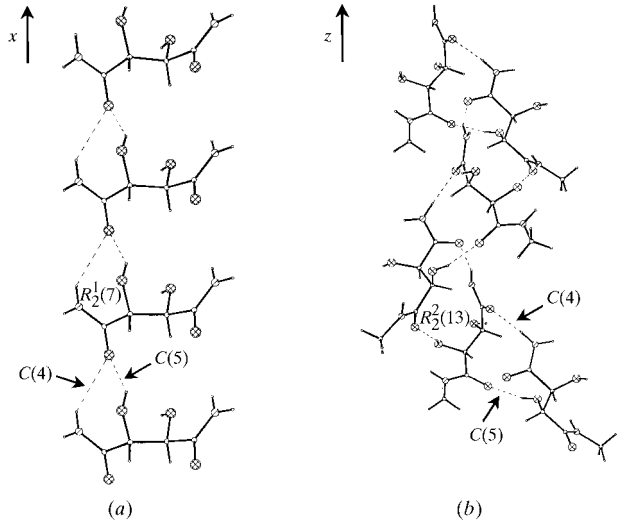

Figure 4
Modification of typical *C*(4) amide chains (molecules aligned head to head) by the presence of hydrogen bonds formed by hydroxyl substituents: (*a*) N—H_{trans}···O═C, *C*(4) amide chain formed by molecules related by approximately 5 Å translation, accompanied by OH···O═C, *C*(5) chain [$R_2^1(7)$ binary pattern (HN11)]; (*b*) N—H_{cis}···O═C, *C*(4) amide chain along 4_1 screw axis accompanied by OH···O═ C, *C*(5) chain [$R_2^2(13)$ binary pattern (HN12)].

Table 4
Hydrogen-bond geometry, space-group symmetry and unit-cell dimensions of (*R*,*R*)-tartaric acid esters and amides.

Intramolecular hydrogen bonds have been marked with asterisks; carbon···oxygen hydrogen bonds have been written in italic; C—H, N—H and O—H distances have been standardized to values of 1.10, 1.03 and 0.97 Å, respectively.

Compound		*D*···*A* (Å)	H···*A* (Å)	*D*—H···*A* (°)	Symmetry operations on *A*	Space group and cell parameters
HOH1	O2—H2O···O1*	2.700 (1)	2.32	103		$P2_12_12_1$
m.p. = 444–445 K	N4—H42···O3*	2.653 (2)	2.21	104		*a* = 5.9556 (5) Å
D/*A* = 5/5	O2—H2O···O4	2.721 (1)	1.85	149	$-\frac{1}{2}-x,-1-y,-\frac{1}{2}+z$	*b* = 8.0972 (5) Å
	O3—H3O···O4	2.780 (2)	1.81	176	$-x,\frac{1}{2}+y,-\frac{1}{2}-z$	*c* = 11.8960 (8) Å
	O10—H10···O2	2.667 (1)	1.74	160	$1+x,y,z$	
	N4—H41···O1	3.267 (2)	2.35	148	$-\frac{1}{2}-x,-1-y,\frac{1}{2}+z$	
	N4—H41···O4	3.098 (2)	2.57	112	$-1-x,\frac{1}{2}+y,-\frac{1}{2}-z$	
	N4—H42···O1	3.336 (2)	2.34	163	$-\frac{1}{2}+x,-\frac{1}{2}-y,-1-z$	
	C3—H3···O1	*3.438 (2)*	*2.47*	*146*	$\frac{1}{2}-x,-1-y,\frac{1}{2}+z$	
HOH2	N4—H4···O3*	2.632 (2)	2.15	107		$P2_12_12_1$
H_2O	O2—H2O···O*W*	2.640 (2)	1.67	178	$-x+1,y+\frac{1}{2},-z+\frac{3}{2}$	*a* = 7.301 (1) Å
m.p. = 427–429 K	O3—H3O···O2	2.859 (2)	1.90	171	$-x+1,y-\frac{1}{2},-z+\frac{1}{2}$	*b* = 7.658 (1) Å
D/*A* = 6/6	O10—H10···O4	2.571 (2)	1.61	170	$x-1,y,z$	*c* = 13.855 (2) Å
	O*W*—H1*W*···O1	2.903 (2)	1.94	171	$-x,y-\frac{1}{2},-z+\frac{3}{2}$	
	O*W*—H2*W*···O1	2.851 (2)	2.03	141	$-x+\frac{1}{2},-y+1,z+\frac{1}{2}$	
	O*W*—H2*W*···O2	2.983 (2)	2.19	139	$-x+\frac{1}{2},-y+1,z+\frac{1}{2}$	
	N4—H4···O*W*	3.105 (2)	2.23	141	$x+\frac{1}{2},-y+\frac{1}{2},-z+1$	
	C2—H2···O10	*3.532 (2)*	*2.44*	*141*	$\frac{1}{2}+x,\frac{1}{2}-y,1-z$	
	C3—H3···O3	*3.425 (2)*	*2.44*	*148*	$1-x,-\frac{1}{2}+y,\frac{1}{2}-z$	
HN11	O2—H2O···O3*	2.823 (3)	2.44	103		$P2_12_12_1$
m.p. = 478–480 K	N1—H12···O2*	2.733 (3)	2.32	103		*a* = 4.9250 (6) Å
D/*A* = 6/4	N4—H42···O3*	2.575 (3)	2.11	105		*b* = 10.060 (1) Å
	O2—H2O···O1	2.776 (3)	1.91	148	$1+x,y,z$	*c* = 12.224 (2) Å
	O3—H3O···O1	2.701 (3)	1.75	166	$\frac{1}{2}+x,-\frac{1}{2}-y,-1-z$	
	N1—H11···O3	3.100 (3)	2.47	119	$-\frac{1}{2}+x,-\frac{1}{2}-y,-1-z$	
	N1—H12···O1	3.233 (3)	2.47	130	$1+x,y,z$	
	N1—H12···O4	3.072 (3)	2.33	128	$-\frac{1}{2}-x,-y,-\frac{1}{2}+z$	
	N4—H41···O4	2.867 (3)	1.86	166	$\frac{1}{2}+x,-\frac{1}{2}-y,-z$	
	N4—H42···O2	3.105 (3)	2.25	139	$-x,-\frac{1}{2}+y,-\frac{1}{2}-z$	
HN12	N1—H12···O2*	2.658 (3)	2.13	109		$P4_12_12$
m.p. = 475–477 K	N4—H4···O3*	2.577 (3)	2.10	106		*a* = 10.594 (1) Å
	N1—H12···O2	2.975 (3)	2.08	144	$1-y,1-x,-\frac{1}{2}-z$	*b* = 10.594 (1) Å
	O2—H2O···O4	2.722 (2)	1.76	171	$1+y,x-1,-z$	*c* = 13.771 (4) Å
	N1—H11···O1	2.837 (3)	1.84	162	$\frac{1}{2}+y,\frac{3}{2}-x,-\frac{1}{4}+z$	
	O3—H3O···O4	2.740 (2)	1.87	148	$\frac{1}{2}+y,\frac{3}{2}-x,-\frac{1}{4}+z$	
	C2—H2···O3	*3.138 (2)*	*2.46*	*118*	$\frac{1}{2}+x,\frac{1}{2}-y,-\frac{1}{4}-z$	
HN13	O3—H3O···O4*	2.620 (2)	2.17	106		$P2_1$
H_2O	N1—H12···O2*	2.695 (2)	2.28	102		*a* = 7.495 (2) Å
m.p. = 418–421 K	O2—H2O···O1*W*	2.716 (2)	1.76	169	$1-x,-\frac{1}{2}+y,1-z$	*b* = 8.517 (2) Å
D/*A* = 6/5	O3—H3O···O1*W*	3.078 (3)	2.39	127	$2-x,-\frac{1}{2}+y,1-z$	*c* = 7.727 (2) Å
	O1*W*—H1*W*···O1	2.724 (2)	1.76	175	$x,1+y,z$	β = 109.90 (2)°
	O1*W*—H2*W*···O4	2.752 (2)	1.79	169		
	N1—H11···O2	3.102 (2)	2.18	148	$1-x,-\frac{1}{2}+y,-z$	
	N1—H12···O1	3.040 (2)	2.09	152	$1-x,\frac{1}{2}+y,-z$	
	*C41—H413···O4**	*2.739 (3)*	*2.28*	*103*		
	C3—H3···O4	*3.389 (3)*	*2.37*	*153*	$2-x,-\frac{1}{2}+y,1-z$	
	C42—H422···O1W	*3.454 (3)*	*2.48*	*147*	$x,-1+y,z$	
HN22	N1—H1···O2*	2.599 (3)	2.13	106		$P2_12_12_1$
H_2O	N4—H4···O3*	2.575 (3)	2.10	106		*a* = 5.094 (1) Å
m.p. = 471–473 K	O3—H3O···O1*W*	2.664 (3)	1.74	158		*b* = 11.243 (2) Å
D/*A* = 6/5	O2—H2O···O2	2.712 (1)	1.77	163	$\frac{1}{2}+x,\frac{1}{2}-y,1-z$	*c* = 16.295 (4) Å
	O1*W*—H1*W*···O1	2.799 (3)	1.90	153	$-\frac{1}{2}+x,-\frac{1}{2}-y,1-z$	
	O1*W*—H2*W*···O1	2.769 (4)	1.82	166	$-1+x,y,z$	
	N1—H1···O4	3.129 (3)	2.16	156	$-\frac{1}{2}+x,\frac{1}{2}-y,1-z$	
	N4—H4···O4	2.886 (3)	2.01	141	$-1+x,y,z$	
	C2—H2···O2	*3.053 (3)*	*2.44*	*114*	$\frac{1}{2}+x,\frac{1}{2}-y,1-z$	
	C2—H2···O3	*3.286 (3)*	*2.26*	*155*	$1+x,y,z$	
HOM	O3—H3O···O2*	2.766 (2)	2.43	100		$P2_1$
m.p. = 330–333 K	O2—H2O···O1	2.946 (2)	2.00	164	$2-x,\frac{1}{2}+y,2-z$	*a* = 5.654 (2) Å
D/*A* = 2/6	O3—H3O···O1	2.942 (2)	2.03	155	$1-x,\frac{1}{2}+y,2-z$	*b* = 8.450 (1) Å
	*C2—H2···O4O**	*2.836 (2)*	*2.44*	*100*		*c* = 8.437 (2) Å
	C3—H3···O2	*3.393 (3)*	*2.47*	*141*	$1-x,y-\frac{1}{2},2-z$	β = 91.36 (2)°
	C40—H403···O4	*3.493 (3)*	*2.47*	*154*	$1-x,-\frac{1}{2}+y,1-z$	

Table 4 (continued)

Compound		$D\cdots A$ (Å)	$H\cdots A$ (Å)	$D-H\cdots A$ (°)	Symmetry operations on A	Space group and cell parameters
HOM1	N4—H41···O3*	2.634 (3)	2.20	103		$P2_12_12_1$
m.p. = 409–412 K	N41—H411···O31*	2.577 (3)	2.14	103		a = 6.7749 (6) Å
D/A = 4/5	O31—H31O···O2	2.782 (2)	1.85	159		b = 7.6467 (7) Å
	O2—H2O···O41	2.712 (2)	1.76	165	$x, 1+y, z$	c = 27.911 (2) Å
	O3—H3O···O21	2.784 (2)	1.82	171	$1+x, 1+y, z$	
	O21—H21O···O4	2.700 (2)	1.83	148	$-1+x, y, z$	
	N4—H42···O41	3.012 (3)	1.99	173	$\frac{1}{2}+x, -\frac{5}{2}-y, -z$	
	N41—H412···O4	2.840 (3)	1.85	160	$-\frac{1}{2}+x, -\frac{5}{2}-y, -z$	
	N4—H41···O31	3.008 (3)	2.36	120	$\frac{1}{2}+x, -\frac{3}{2}-y, -z$	
	N41—H411···O3	3.209 (3)	2.49	127	$-\frac{1}{2}+x, -\frac{3}{2}-y, -z$	
	C51—H511···O5	*3.442 (4)*	*2.43*	*152*	$-1+x, y, z$	
	C51—H512···O1	*3.454 (4)*	*2.41*	*158*		
HOM3	O2—H2O···O1*	2.682 (5)	2.24	106		$P2_1$
m.p. = 318–321 K	O3—H3O···O4*	2.524 (4)	1.78	131		a = 5.849 (4) Å
D/A = 2/5	O21—H21O···O11*	2.741 (4)	2.42	99		b = 16.245 (9) Å
	O31—H31O···O41*	2.545 (4)	1.94	118		c = 9.653 (7) Å
	O21—H21O···O2	2.800 (4)	1.98	141		β = 90.09 (6)°
	O2—H2O···O11	3.073 (5)	2.56	113		
	O31—H31O···O51	3.081 (4)	2.34	133	$1+x, y, z$	
	C43—H433···O4	*3.325 (5)*	*2.34*	*147*	$1+x, y, z$	
	C21—H21···O41	*3.376 (5)*	*2.38*	*150*	$-1+x, y, z$	
	C31—H31···O4	*3.428 (5)*	*2.39*	*157*	$-1-x, \frac{1}{2}+y, -2-z$	
	C45—H451···O41	*3.204 (5)*	*2.39*	*129*	$-1+x, y, z$	

The pure amide···amide hydrogen bonds, present in various crystal structures of (*R*,*R*)-tartramides, do not appear as single motifs, but rather as constituents of more extensive hydrogen-bonding systems, as illustrated in Figs. 3 and 4. Some of these bonds are rather weak, as judged from the bond distances (Table 4).

3.2.2. OH···OH hydrogen-bond motifs. Two types of secondary hydroxyl···secondary hydroxyl hydrogen-bonded chains can be distinguished: the $C(2)$ chain, joining symmetry-equivalent hydroxyl groups, and $C(5)$ chain (or D if two independent molecules are involved), joining two different hydroxyl substituents. The $C(2)$ chain, built up solely of hydroxyl units, is stabilized by σ-cooperativity (Jeffrey & Saenger, 1991). The motif could be considered as rather uncommon in the investigated series, for it is observed in only one crystal structure (HN22, Fig. 10*c*), except for a homodromic $C_2^2(4)$ OH···OH chain, which is twice the fundamental $C(2)$ motif and which appears in the crystal structure of HOH2 (Rychlewska *et al.*, 1999). The $C_2^2(4)$ pattern forms by combining, on the binary level, two D motifs.

The $C(5)$ secondary hydroxyl···secondary hydroxyl hydrogen-bond motif is present in only one crystal structure (HOH2; Rychlewska *et al.*, 1999), but its analogue, the secondary hydroxyl···secondary hydroxyl D motif, appears in amidoesters HOM1 (Szarecka *et al.*, 1996) and HOM3 (Gawroński *et al.*, 1997), both of which crystallize with two molecules in the asymmetric unit.

Other types of OH···OH chains involve the carboxylic hydroxyl group, acting as a proton donor [$C(5)$ motif, HOH1, Fig. 9*a*] or a water molecule acting as a proton acceptor (D motif, present in all hydrated crystals: HOH2, HN13, HN22). Among the two types of bonds one finds the shortest bonds of all observed in the derivatives studied (Table 4). The latter case reflects a well known observation (Jeffrey, 1994) that a water molecule is a much stronger acceptor than donor. Water, as a donor to the hydroxyl group, appears only in HOH2 where the previously mentioned homodromic $C_2^2(4)$

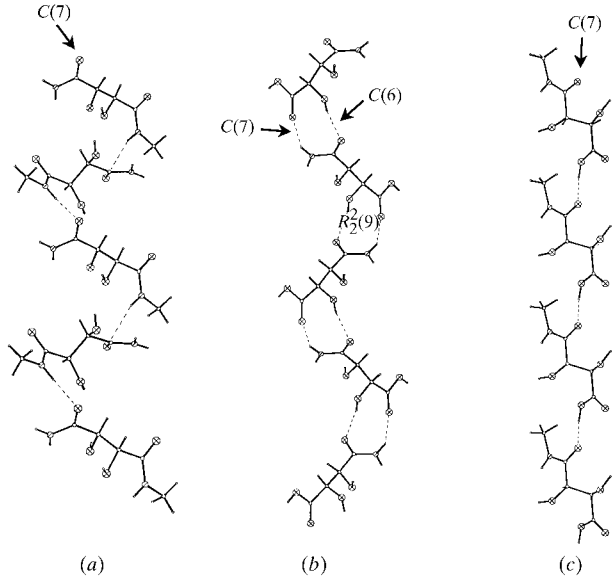

Figure 5
$C(7)$ chains connecting molecules in a head-to-tail mode: (*a*) amide···amide chain (invariably links screw-axis related molecules) observed in HN12; (*b*) an analogous amide···carboxyl chain present in HOH1. The chain is accompanied by OH···O=C, $C(6)$ chain, which results in the binary pattern $R_2^2(9)$; (*c*) carboxyl···amide chain (HOH2), joining molecules related by a unit-cell translation of approximately 7.2 Å, analogous to carboxyl···carboxyl chains present in the parent (*R*,*R*)-tartaric acid and in (*R*,*R*)-hydrogentartrates.

OH···OH chain is formed. Almost invariably, a water molecule acts as a proton acceptor from a secondary hydroxyl group and donates its protons to either carboxyl or amide carbonyls, but not to the ester carbonyl. This results in OH···O*W*—H···O═C hydrogen-bond patterns (*see below*). The O*W*—H···O═C hydrogen bonds which, in hydrated crystals, replace the 'usual' OH···O═C bonds are noticeably longer than the latter ones [average values 2.80 (6) and 2.73 (3) Å, respectively].

In essence, intermolecular OH···OH hydrogen bonds, formed in many different ways as described above, are rather common in the investigated series. Although they are not present in the crystal structure of tartramate (HOM) and the two (*R*,*R*)-tartaric acid diamides (HN11 and HN12), in the first two structures (HOM and HN11) an intramolecular hydroxyl···hydroxyl hydrogen bond exists instead, described by the *S*(5) pattern designator. The secondary hydroxyl···secondary hydroxyl bonds seem characteristic for monoesters which crystallize with two molecules in the asymmetric unit, while the secondary hydroxyl···water hydrogen bonds dominate in derivatives containing monomethyl- or dimethylamide groups. In these crystal structures the hydroxyl functions are used to join together the hydrophilic regions, often with the help of water molecules (HN22, HN13; Figs. 13 and 14).

3.2.3. Mixed amide, carboxyl and hydroxyl hydrogen-bond motifs. Present in all derivatives are hydroxyl···carbonyl hydrogen bonds. The donor might be a secondary hydroxyl group, a carboxylic hydroxyl or a water molecule, and the acceptor an acid, ester or amide carbonyl. The shortest of all the bonds is the carboxylic hydroxyl···amide carbonyl hydrogen bond, present in the crystal structure of HOH2 (Rychlewska *et al.*, 1999). It leads to the formation of a *C*(7) motif (Fig. 5*c*), analogous to the carboxyl···carboxyl chain present in the crystal structure of the parent (*R*,*R*)-tartaric acid (Okaya *et al.*, 1966). The chain links translationally related molecules in a head-to-tail mode, parallel to the crystallographic axis of length 7.301 Å [Table 4; 7.729 Å in (*R*,*R*)-tartaric acid]. The described motif not only appears in crystals of (*R*,*R*)-tartaric acid, but is characteristic of the mode of packing of hydrogen tartrate anions (Marthi *et al.*, 1995, and references therein; Fun & Sivakumar, 1995). Considering this, and certain other analogies between the crystal structure of HOH2 and (*R*,*R*)-tartaric acid (Rychlewska *et al.*, 1999), we may conclude that in *N*-methyltartramic acid (HOH2) the packing is governed by the carboxylic rather than amide functional groups.

A secondary hydroxyl group acting as a donor to carbonyl oxygen forms both intra- and intermolecular hydrogen bonds. The intramolecular motif is invariably *S*(5), while the intermolecular motif is either the $R_2^2(12)$ dimer, formed between two β-hydroxycarbonyl moieties related by the twofold symmetry axis (HN12, Fig. 3*c*), or the *C*(5) or *C*(6) chain (the dimensionality of the chain motif depending on whether the hydroxyl comes from the same or the other half of the molecule). Intermolecular secondary hydroxyl···carbonyl bonds are much stronger when the acceptor is the amide carbonyl rather than the ester carbonyl, the average donor···acceptor distances being 2.73 (3) and 2.99 (6) Å, respectively. The secondary hydroxyl···amide carbonyl chains often accompany typical amide chains, as illustrated in Figs. 4(*a*) and (*b*). Of the two types of bonds, the hydroxyl···carbonyl bonds seem to be stronger. However, an analysis of the various packing patterns formed by derivatives containing a primary α-hydroxyamide group seems to indicate that the OH···O═C motifs follow the patterns dictated by the amide groups (Figs. 4 and 5).

The NH···OH hydrogen bonds almost exclusively engage secondary hydroxyl groups as acceptors, the only exception being the NH···O*W* hydrogen bond observed in HOH2. The bonds are formed in compounds containing

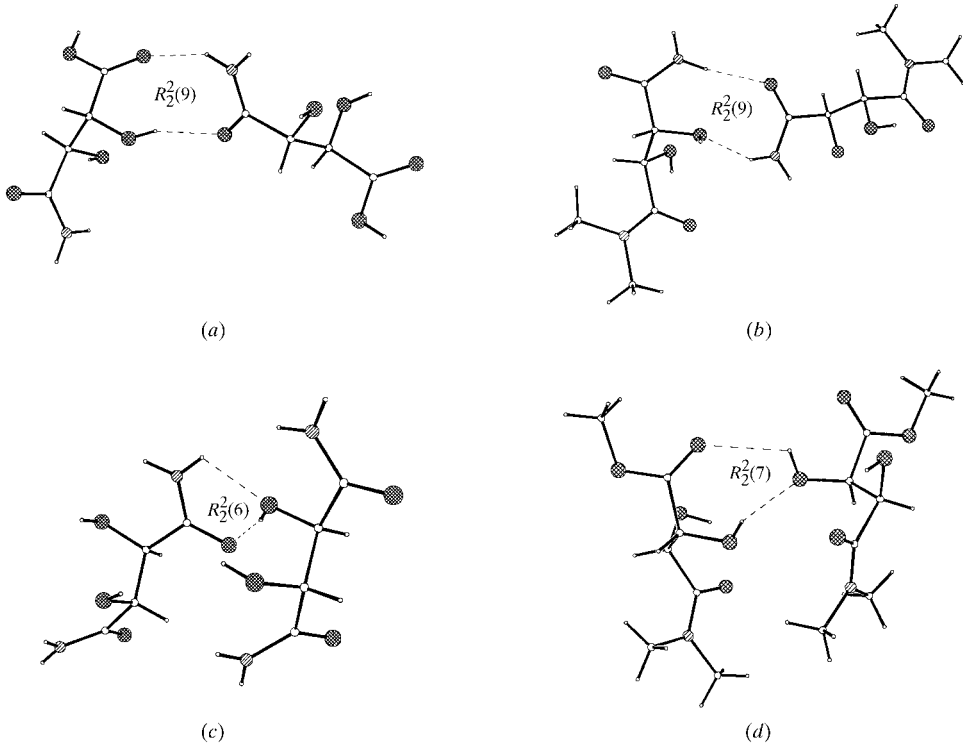

Figure 6
Ring hydrogen-bond patterns formed by two complementary groups of dual donor/acceptor functionality: (*a*) α-hydroxycarboxyl···amide $R_2^2(9)$ pattern (HOH1); (*b*) α-hydroxyamide···amide $R_2^2(9)$ pattern (HN13); (*c*) amide···hydroxyl $R_2^2(6)$ pattern (HN11); (*d*) α-hydroxyamide···hydroxyl $R_2^2(7)$ pattern (HOM3).

primary amide substituents (HN11, HN12, HN13 and HOM1). Intramolecular NH(*trans*)···OH hydrogen bonds create *S*(5) motifs. Intermolecular NH···OH hydrogen bonds lead to either $R_2^2(10)$ dimers (Fig. 3*b*), or to *C*(5) or *C*(6) chains. The NH···OH chains, when combined on a binary level with other types of hydrogen-bond motif, constitute part of a ring system, as illustrated in Figs. 6(*b*) and (*c*).

The rather unusual $R_2^2(10)$ ring motif might be considered as a characteristic of optically active tartramides, since it is formed between two α-hydroxyamide moieties (HN12, Fig. 3*b*, right). The two units are related by the twofold symmetry axis. Two independent molecules in HOM1 form an analogous dimer (Fig. 3*b*, left). In fact, the two molecules are topologically very similar and might be expected to aggregate in a similar way. However, the mode in which the dimers are further extended in the crystal differs in the two compounds. While in HOM1 the dimer is fused (*i.e.* contains one chemical bond in common) with a typical amide $R_2^2(8)$ dimer (Fig. 14*a*), in HN12 the $R_2^2(10)$ dimer shares the N—H···OH hydrogen bond with the neighbouring ring, the N—H(*cis*) hydrogen being involved instead in building the *C*(4) chain which joins molecules related by the 4_1 screw axis (Fig. 4*b*). The intermolecular NH···OH bonds are long [average value 3.08 (8) Å] and nonlinear, so they seem to play rather a supportive than a decisive role in molecular association. In general, amide H atoms, N—H(*trans*) in particular, commonly form more than one hydrogen bond, thus participating in three- or four-centre bonds. Being constituents of the three-centre bonds, the NH···O bonds often depart significantly from linearity.

Hydroxyl groups proximal to primary or secondary amide residues are always engaged in intramolecular hydrogen bonds as acceptors. Moreover, hydroxyl groups that are proximal to primary amides almost invariably act as acceptors of intermolecular hydrogen bonds from the N—H group. The proton-accepting affinity of hydroxyl substituents steadily decreases if the neighbouring amide group is singly or doubly methylated.

The three major types of intramolecular hydrogen bonds that are observed in the crystal structures studied always led to the formation of *S*(5) motifs. These include the following.

(i) An internal hydrogen bond between the secondary hydroxyl as a donor and the nearest acid, ester or amide oxygen function as an acceptor (Fig. 2*a*). In α-hydroxy acid and α-hydroxy ester moieties the acceptor might be one of two

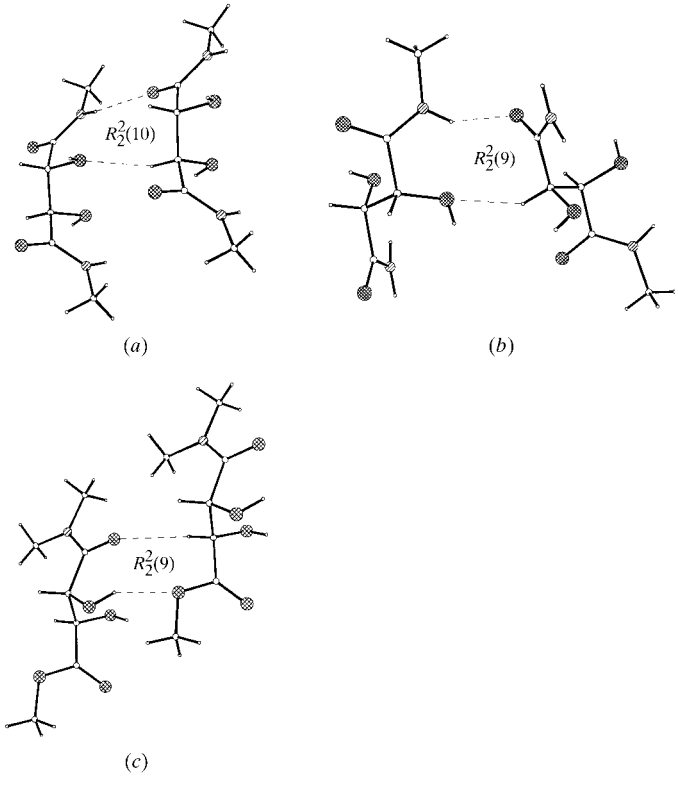

Figure 7
Rings, analogous to those shown in Fig. 6, but involving C(β)—H/CO and C(α)—H/CO fragments acting as donor/acceptor groups: (*a*) α-hydroxyamide···C(β)—H/CO, $R_2^2(10)$ pattern (HN22); (*b*) α-hydroxyamide···C(α)—H/CO $R_2^2(9)$ pattern (HN12); (c) α-hydroxyamide···C(α)—H/CO, $R_2^2(9)$ pattern (HOM3). Note the change of conformation, from *a* to *s*, accompanying the replacement of a secondary by a tertiary α-hydroxyamide, and connected with it a change of the α-hydroxyl function from acceptor (*b*) to donor (*c*).

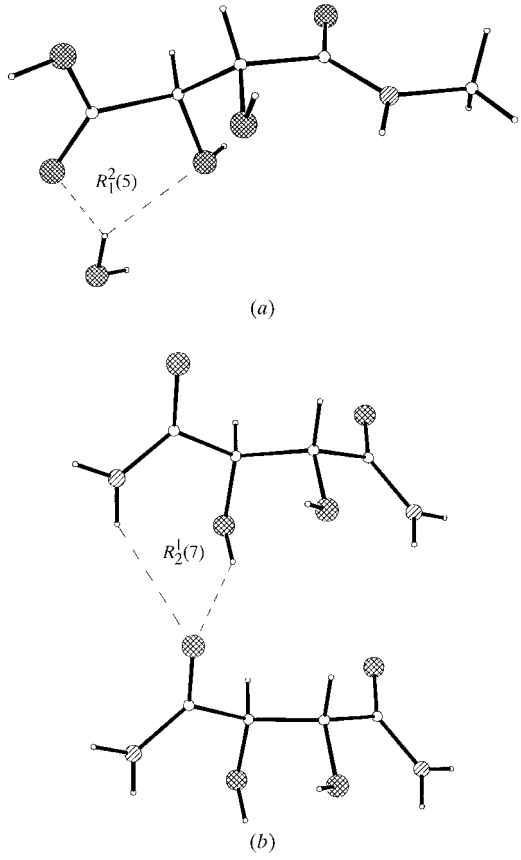

Figure 8
Ring patterns: (*a*) the $R_1^2(5)$ pattern (HOH2) with the α-hydroxycarboxyl group functioning as a double acceptor (the donor is the water solvent molecule). Note that the *a* conformation adopted by primary and secondary α-hydroxyamide groups precludes the double acceptor function of these fragments; (*b*) the $R_2^1(7)$ pattern with the α-hydroxyamide moiety functioning as a double donor (HN11).

O atoms, although the OH···O=C hydrogen bond prevails. This type of intramolecular hydrogen bond is also formed in tertiary amides which adopt the *s* conformation of the α-hydroxy-*N*,*N*-dimethylamide moiety (HN13, HOM3; Gawroński *et al.*, 1997) and is precluded in primary and secondary amides due to their pronounced tendency to adopt the *a* conformation of the α-hydroxyamide fragment (*see above*).

(ii) An internal hydrogen bond between N—H as a donor and secondary OH, from the same half of the molecule, as an acceptor (Figs. 3*a*, *b* and *c*). Formation of such a bond requires a planar α-hydroxyamide group with the C—N bond proximal and C=O distal to the hydroxyl O atom. The observed conformational preferences of primary and secondary amides (*see above*) favour the formation of this type of hydrogen bond.

(iii) An internal hydrogen bond between two vicinal hydroxyl groups, as found in the crystal structures of HN11 (Gawroński *et al.*, 1997) and HOM (Rychlewska *et al.*, 1997), see Table 4. Usually, although not always, these intramolecular interactions occur as minor components of three- and four-centre hydrogen bonds, so they must be weak. However, the extent to which they are preserved in the solid state compared with the isolated state (Gawroński *et al.*, 1997; Hoffmann *et al.*, 1999; Polavarapu *et al.*, 1987) is quite high. The observed intramolecular interactions involve only proximal groups, thus no rings other than five-membered are formed. In the graph-set notation all these hydrogen-bond types might be described by one type of designator, *S*(5). This contrasts with the situation in isolated tartramides and tartramides in nonpolar solutions, where, as a result of the presence of the internal hydrogen bonds between β hydroxyls and carbonyl O atoms, six-membered rings, described by a *S*(6) pattern designator, are formed (Gawroński *et al.*, 1997; Hoffmann *et al.*, 1999).

Besides imposing some rigidity on the molecule, intramolecular hydrogen bonds might play a key role in preserving the hydrogen-bond cooperativity in the system. In the studied tartaric acid derivatives, hydrogen-bond functional groups are separated by a single covalent bond. Therefore, the presence of intramolecular hydrogen bonds joining proximal groups permits the formation of one-, two- or three-dimensional patterns composed exclusively of hydrogen bonds and stabilized by both σ- and π-cooperativity (for example, see Fig. 9*b*).

3.2.4. Higher-level hydrogen-bond patterns characteristic for the crystal structures of monoamides and diamides of (*R*,*R*)-tartaric acids. Although in many of the crystal structures of tartramides typical amide aggregation patterns do appear, they are almost invariably accompanied by other motifs that might be considered as playing a supportive role with respect to the amide pattern. Accordingly, in tartramides, an analogue of a typical $R_2^2(8)$ amide dimer would be the set of three rings $S(5)R_2^2(8)S(5)$ that share together the N—C amide bonds (Fig. 3*a*). The global energy of the three-ring pattern, described on the quaternary level as $R_4^4(14)$, is much lower than that of the other α-hydroxyamide dimer, the $R_2^2(10)$ ring (Fig. 3*b*). The energy difference between the two patterns amounts to approximately 29.3 kJ mol^{-1} (Szarecka *et al.*, 1999).

Similarly, the formation of the characteristic amide *C*(4) chains is usually supplemented by *C*(5) or *C*(6) hydroxyl···carbonyl or amide···hydroxyl hydrogen-bonded chains (Figs. 4*a* and *b*, and 5*b*). This necessarily leads to various ring systems on the binary and higher levels. Particularly rich in ring patterns are derivatives containing primary amide groups (HOH1, HN11, HN12, HN13 and HOM1). Inspection of binary graph sets reveals hydrogen-bond ring patterns that involve α-hydroxycarboxyl, α-hydroxyamide, α-hydroxyester, amide and hydroxyl functional groups [graph set designators $R_2^2(9)$, $R_2^2(6)$ and $R_2^2(7)$], see Figs. 6(*a*)–(*d*). Patterns of this type are formed by taking advantage of the dual hydrogen-bond functionality of all the above-mentioned groups. All these

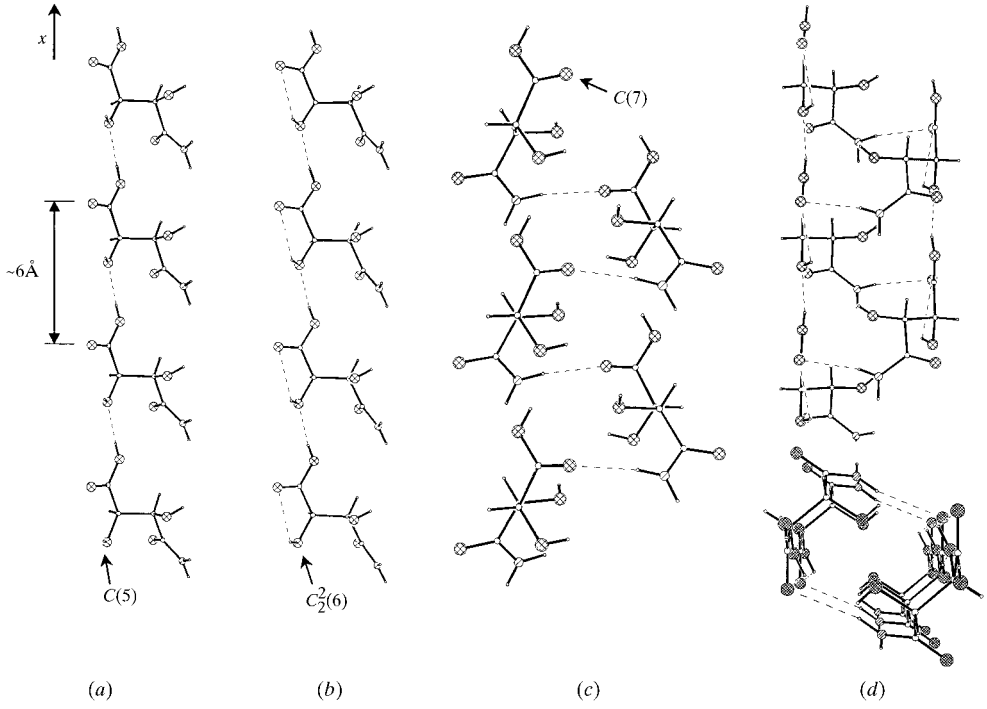

Figure 9
Chain motifs, aligned along the 6 Å screw axis, constituting the helix in HOH1. (*a*) *C*(5) carboxyl···hydroxyl chain (molecules aligned head-to-head); (*b*) the same chain, but with the intramolecular hydrogen bond accounted for [the $C_2^2(6)$ carboxyl···α-hydroxycarboxyl chain]; (*c*) *C*(7) amide···carboxyl chain (molecules aligned head-to-tail); (*d*) the resulting helix, side view (top) and view along the axis of the helix (bottom).

arrangements were calculated to be stable in the isolated state and in liquid media (Szarecka *et al.*, 1999, 2000). Methyl substitution limits the number of hydrogen-bond donor groups. In such cases, the C*—H group (associated with a chiral centre) takes the role of hydrogen-bond donor. The linking α-hydroxyamide group is replaced by the C(β)—H/CO fragment, which is similar in shape and function. The $R_2^2(10)$ ring formed (Fig. 7*a*) mimics the $R_2^2(10)$ α-hydroxyamide dimer (Fig. 3*b*). Similarily, the C(α)—H/CO group can replace the *cis*-amide linkage in its dual hydrogen-bond functionality and form, together with the α-hydroxyamide group, a nearly identical $R_2^2(9)$ pattern. This is shown in Figs. 7(*b*) and (*c*), where the C(α)—H/CO fragment is bound to, respectively, secondary and tertiary α-hydroxyamide functions. Comparison of the two figures illustrates the different roles of the α-hydroxyl group in hydrogen-bond formation, depending on the conformational preferences of the two amide functions. In all these hydrogen-bonded rings shown in Figs. 6 and 7, proximal functional groups that constitute α-hydroxycarboxyl, α-hydroxyamide, amide or α-hydroxyester moieties are combined *via* the linking group that displays complementary donor/acceptor ability.

Other ring systems that are formed on a binary level involve an α-hydroxycarboxyl group acting as a double acceptor [$R_1^2(5)$ pattern designator, Fig. 8*a*] or an α-hydroxyamide group acting as a double donor [$R_2^1(7)$ pattern designator, Fig. 8*b*]. The $R_1^2(5)$ pattern might be considered as analogous to the *S*(5) motif formed between the hydroxyl group and the oxygen of the proximal carboxyl or ester group. Jeffrey & Saenger (1991) have described this type of bonding as a mediated intramolecular hydrogen bond. The motif is not only common among the tartaric acid derivatives and salts (for example, see Bootsma & Schoone, 1967; Carlström, 1973; Duesler *et al.*, 1984*a*,*b*), but is also present in other systems containing either the α-hydroxycarboxylate moiety (Flippen, 1973; Larsen & Marthi, 1994; Foster & James, 1983; Schouten *et al.*, 1994) or the dicarboxylate moiety, as in oxalic acid (Bernstein *et al.*, 1994). In some of the cases cited, the role of the mediator is played by the solvent water molecule (Flippen, 1973) or by a hydroxyl group from a cation (Carlström, 1973). The motif can also be viewed as analogous to chelate rings formed by tartrate ligands (Gawroński & Gawrońska, 1999). It might be interesting to note that such a pattern cannot be present in the investigated crystal structures of primary and secondary (*R*,*R*)-tartramides nor in any aliphatic α-hydroxyamides (Kennard & Allen, 1993), because of the strong preference of this group of compounds to adopt *antiplanar* rather than *synplanar* orientations of the carbonyl/α-hydroxyl groups. Quantum chemical calculations, carried out on the MP2/6-311++G**//RHF/6-311++G* level for model systems containing hydroxyacetic acid or hydroxyacetamide as the basic constituents of the $R_1^2(5)$ pattern, seem to mirror our observations. While model systems containing hydroxyacetic acid are stable and their stability increases considerably in liquid media, in particular those of high polarity (Rychlewska *et al.*, 1999), models with hydroxyacetamide as the basic constituent are not stable, and, after geometry optimization, evolve to other ring systems (Rychlewski & Szarecka, 2000). Similarly, the $R_2^1(7)$ pattern, formed when the α-hydroxyamide moiety acts solely as a hydrogen-bond donor group, observed in the crystal structure of HN11 (Figs. 4*a* and 8*b*) has turned out to be unstable in the isolated state (Rychlewski & Szarecka, 2000).

Combination of two chain motifs propagating in the same direction, of which one joins the molecules head-to-head, while the other head-to-tail, leads in certain circumstances to arrangements that resemble polypeptide helices (Figs. 9*d*, 10*d* and 11*d*). For example, in the crystal structure of HOH1 (Fig. 9), molecules related by a unit translation of 5.9556 (5) Å are connected by hydrogen bonds in a head-to-head fashion forming the *C*(5) chain motif. On a binary level, the chain can be viewed as consisting of two motifs: *C*(5) and *S*(5), which combine to give a $C_2^2(6)$ infinite homodromic chain (Fig. 9*b*), stabilized by both σ- and π-bond cooperativity (this might be the cause of the carboxylic hydroxyl···secondary hydroxyl hydrogen bond being relatively short, Table 4). Topologically, the $C_2^2(6)$ chain might be viewed as analogous to the amide *C*(4) chain joining molecules related by approximately 5 Å translation (compare Figs. 9*b*

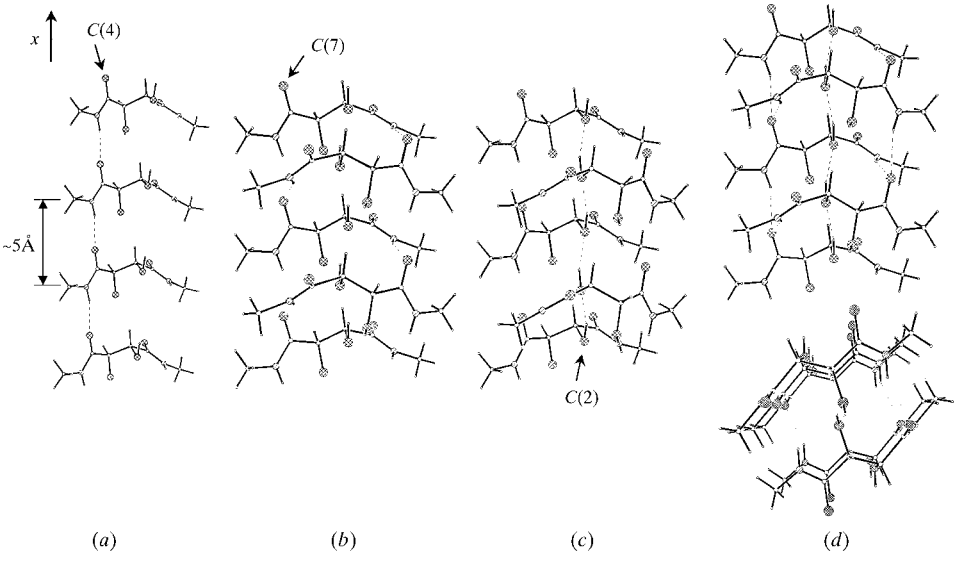

Figure 10
Chain motifs, aligned along the 5 Å screw axis, constituting the helix in HN22. (*a*) *C*(4) amide chain (molecules aligned head-to-head); (*b*) *C*(7) amide chain (molecules aligned head-to-tail); (*c*) homodromic hydroxyl *C*(2) chain that runs inside the helix; (*d*) the resulting helix, side view (top) and view along the axis of the helix (bottom).

with 10*a* and 11*a*). The length of the carboxylic group alone is too small to allow the formation of carboxylic chains analogous to the *C*(4) amide chains. However, a planar, intramolecularly bonded α-hydroxycarboxyl group displays suitable dimensions for joining, by hydrogen bonds, molecules related by translation in a head-to-head fashion. Thus, the presence of the intramolecular hydrogen bond between secondary hydroxyl and proximal carboxyl groups helps to extend carboxyl dimensions to a value required to form hydrogen bonds between translationally related molecules (approximately 6 Å) and to maintain cooperativity in the hydrogen-bond chain. The *C*(5) chain [or in other words the $C_2^2(6)$ chain] is accompanied by the *C*(7) chain (Fig. 9*c*), in which the amide group is a donor and the carboxylic carbonyl is an acceptor. In the chain, the hydrogen-bonded molecules which are related by a twofold screw axis are joined in a head-to-tail fashion. The hydrogen bonds are almost perpendicular to the direction of the propagation of the chain. Combination of these two chains leads to the helical arrangement of hydrogen-bonded molecules that resembles a polypeptide helix, in which the peptide bonds have been replaced by the amide···carboxyl hydrogen bonds (Fig. 9*d*).

Helices, analogous to the one described above but built up solely of amide chains, can be found in the crystal structures of HN22 (Fig. 10) and HN11 (Fig. 11). In HN22, the helix is formed by combining together a *C*(4) chain (Fig. 10*a*) which joins molecules (along *x*) related by a unit-cell translation of 5.094 (1) Å (N—H_{trans}, as the donor, molecular alignment head-to-head) and a *C*(7) chain (Fig. 10*b*), running in the same direction, formed by molecules related by a twofold screw axis (N—H_{trans}, as the donor, molecular alignment head-to-tail). Inside the helix, presented in Fig. 10(*d*), one finds a homodromic *C*(2) chain, formed by secondary hydroxyl groups joined together by hydrogen bonds, running also in the *x* direction (Fig. 10*c*). In HN11 a more extended helical arrangement of molecules is present and in this structure the helix is formed by combining two *C*(4) chains – one joining molecules related by a unit-cell translation of 4.9250 (6) Å (N—H_{trans} as a donor, Fig. 11*a*) and the other, formed at the other end of the molecule, joining molecules related by a twofold screw axis (N—H_{cis} as a donor, Fig. 11*b*). Propagating in the same direction are also two *C*(6) chains (formed by NH···β-OH and β-OH···O=C bonds), which combine together to form a $R_2^2(6)$ ring (Fig. 11*c*). The helical chain of the $R_2^2(6)$ rings mediates in connecting neighbouring amide helices, as shown in Fig. 11(*d*). In the crystal structure of HN22 (Fig. 10), such linking between the amide helices is precluded because of the presence of methylamide substituents at both ends of the molecule and, consequently, at both sides of the helix (Fig. 10*d*). Therefore, the connection between neighbouring helices is realised *via* mediating water molecules in a way depicted in Fig. 13(*c*).

Present in all but one (HN12) of the crystal structures are arrangements that combine the OH···OH···O=C hydrogen bonds (Fig. 12). The patterns are formed in many different ways, depending on the source of hydroxyl groups and the positions of the carbonyl functions (proximal or distal to the hydroxyl). In the majority of cases it leads to the formation of chains described by $C_2^2(n)$ pattern designators (*n* varies from 6 to 9), but the ring analogue, the $R_2^2(7)$ pattern, is also present (HOM3, Fig. 6*d*). The many variations of the chain patterns include a secondary hydroxyl···secondary hydroxyl hydrogen bond that is formed between two independent molecules [HOM1, pattern designator $C_2^2(7)$, Fig. 12*a*] or a secondary hydroxyl···secondary hydroxyl intramolecular hydrogen bond [HN11, HOM, Fig. 12*b*, pattern designator $C_2^2(7)$]. In hydrates, the combination involves secondary hydroxyl···water hydrogen bonds, resulting in either $C_2^2(7)$ or $C_2^2(8)$ patterns. The patterns are observed in all hydrated derivatives and are represented in Fig. 12(*c*) for the HN22 crystal structure. Moreover, one of the participating hydroxyl groups can be provided by a carboxyl substituent, as in HOH1, which leads to the $C_2^2(9)$ pattern (Fig. 12*d*). Also belonging to this category is the homodromic $C_2^2(6)$ chain, illustrated in Fig. 9(*b*), which has the OH···O=C bond as an intramolecular constituent.

In *N*-monomethylamide derivatives (HOH2, HN22), the OH···OH···O=C chain described thus far constitutes part of a ring of dimensionality 12 (Figs. 13*a* and *c*). The ring always contains at least one water molecule and a β-hydroxycarbonyl unit. A similar cyclic arrangement can be found in the crystal structure of the parent (*R*,*R*)-tartaric acid (Fig. 13*b*), where one of the hydroxyl substituents plays the role of water in the linkage. This seems to indicate a carboxylic rather than amide origin of this pattern. The ring might be viewed as analogous to the $R_2^2(12)$ dimer formed

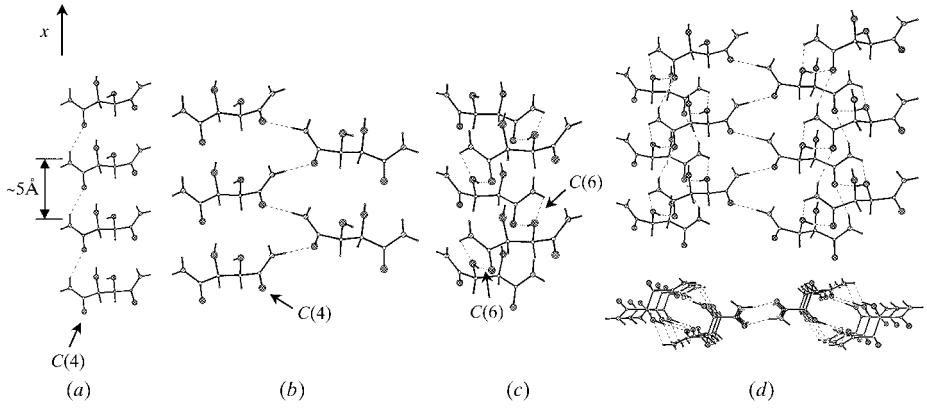

Figure 11
Chain motifs, aligned along the 5 Å screw axis, constituting the helix in HN11. (*a*) *C*(4) amide chain (translationally related molecules aligned head-to-head); (*b*) *C*(4) amide chain (screw-axis-related molecules aligned head-to-head); (*c*) two supportive *C*(6) chains; (*d*) the resulting helix, side view (top) and view along the axis of the helix (bottom).

between two β-hydroxycarbonyl groups in HN12 (Fig. 3*c*). A topologically similar ring is formed in HN13 (Fig. 13*d*), although in this crystal structure an amine group has been accommodated as one of the linkages. Accordingly, the role of the β-hydroxycarbonyl fragment has been switched from donor/acceptor to double acceptor. All ring patterns depicted in Figs. 13(*a*)–(*d*) have the same dimensionality of 12, although on different levels. This might be viewed as an indication that in order to join together the β-hydroxycarbonyl fragment, the mediating group(s) should consist of six to seven atoms connected by either covalent or hydrogen bonds.

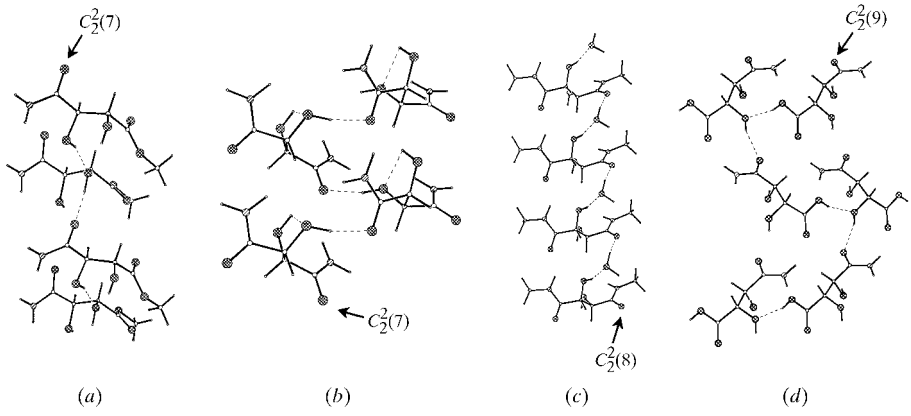

Figure 12
Patterns involving OH···OH···O=C fragments: (*a*) $C_2^2(7)$ pattern, observed in HOM1, involving two secondary hydroxyl groups; (*b*) $C_2^2(7)$ pattern (HN11) involving intramolecular hydrogen bonds between vicinal OH groups; (c) $C_2^2(8)$ pattern which includes water molecules (HN22); (*d*) $C_2^2(9)$ pattern involving the carboxylic hydroxyl group (HOH1).

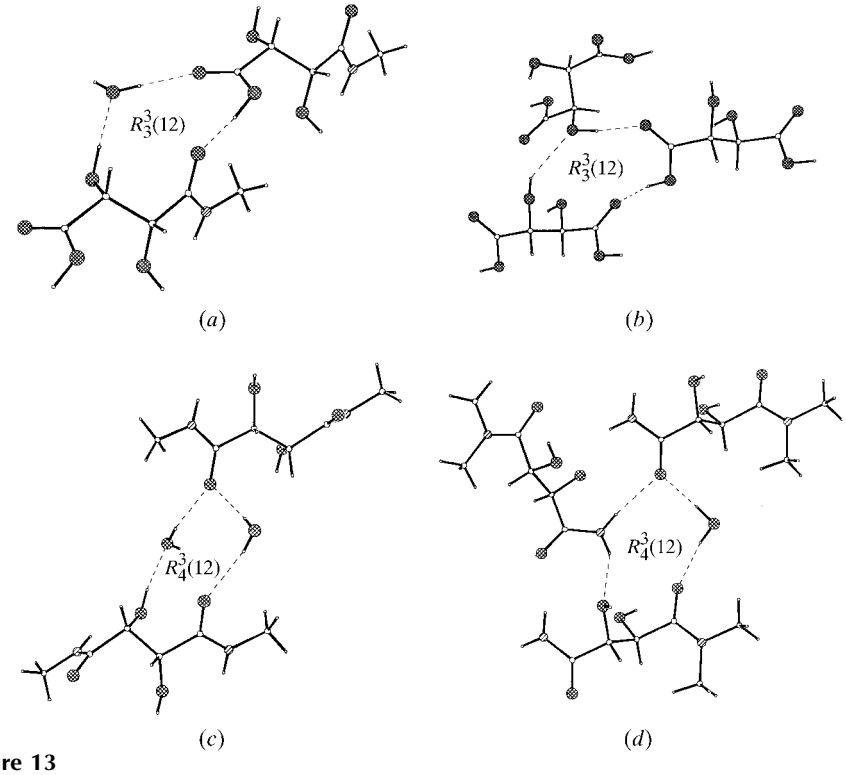

Figure 13
Ring patterns which are formed by joining together the β-hydroxycarbonyl moiety observed in hydrated derivatives and in the parent tartaric acid. (*a*) HOH2, (*b*) *R*,*R*-tartaric acid (adopted from Okaya *et al.*, 1966), (*c*) HN22 and (*d*) HN13.

3.3. Packing of (*R*,*R*)-tartaric acid esters and amides

Substitution by methylester or methylamide groups leads to packing problems connected with the steric bulk of the methyl substituents. Conformationally flexible α-hydroxyester residues overcome this obstacle by switching their conformation around the Csp^3-Csp^2 bond by 180° (HOM, Rychlewska *et al.*, 1997; HOM1, Szarecka *et al.*, 1996) and/or by increasing the number of molecules in the asymmetric unit (HOM1, Szarecka *et al.*, 1996; HOM3, Gawroński *et al.*, 1997). On the other hand, conformationally more rigid α-hydroxy-*N*-methylamide and α-hydroxy-*N*,*N*-dimethylamide derivatives (HOH2, Rychlewska *et al.*, 1999; HN13, Gawroński *et al.*, 1997; HN22, this work) use water molecules for this purpose (Table 4). This is illustrated in Fig. 14 by comparing the crystal structures of HOM1 and HN13. The two compounds form topologically similar infinite ribbons in the crystal lattice, consisting of rings having one amide bond in common. Methyl groups are situated on both sides of the ribbons (Figs. 14*a* and *b*). Both patterns have the same $R_4^4(16)$ designator, on quaternary and binary levels, respectively. In HOM1, the ribbons are further extended into infinite layers by means of the secondary hydroxyl···secondary hydroxyl hydrogen bonds (Fig. 14*c*). The steric hindrance due to the methyl substituents is overcome by the presence of two molecules in the asymmetric unit which adopt conformations differing in rotation around the Csp^3-Csp^2 bond by 180°. In contrast to this, the steric hindrance in HN13, caused by the presence of the *N*,*N*-dimethylamide substituent, cannot be overcome in an analogous way owing to the well defined conformational preferences of the α-hydroxy-*N*,*N*-dimethylamide moiety (invariably *s*, *see above*). Therefore, in this crystal structure further extension of the hydrogen-bond network is accomplished by means of crystal water molecules that easily fit into voids created by dimethylamide substituents (Fig. 14*d*). In this context it might be worth mentioning that the combination of carboxyl/*N*,*N*-dimethylamide (HOH3) and *N*-methylamide/*N*′,*N*′-dimethylamide (HN23) substituents leads to derivatives

which are liquid at room temperature (Gawroński *et al.*, 1997). Difficulties in arranging these molecules in the three-dimensional lattice might arise from the steric hindrance and conformational disparity of the two halves that constitute the particular derivative. The relative size of the two substituents might also play a significant role due to the well known tendency for molecules to crystallize with separated hydrophilic and hydrophobic regions. Concentration of methyl substituents outside two-dimensional layers (HOM, Rychlewska *et al.*, 1997; HOM1, Szarecka *et al.*, 1996) and one-dimensional columns (HOM3, Gawroński *et al.*, 1997) is particularly obvious in the methylester derivatives. The layers are perpendicular to the longest crystallographic axis and the thickness of the layer is approximately 7–8 Å. In these derivatives, the amount of CH···O hydrogen bonds significantly increases (Table 4). Since these bonds often involve methyl groups as donors, their role is to join adjacent hydrophilic layers or columns. It might be interesting to note that in HOM3, the compound with the lowest melting point of 318–321 K (Table 4), the degree of C—H···O hydrogen bonding is the highest in the investigated series. At the same time, one of the four hydroxyl groups present in the asymmetric unit is engaged exclusively in an intramolecular hydrogen bond.

Finally, a mention should be made about the macroscopic behaviour of the investigated crystals. The values of melting points vary from over 473 to *ca* 323 K (Table 4) and decrease in the order primary amides > secondary amides > acids > tertiary amides > esters. This matches quite well the order of decreasing hydrogen-bond donor-to-acceptor ratio calculated for the content of the asymmetric unit (Table 4). Following this trend, monomethyl (*R*,*R*)-tartrate (*X* = OH, *Y* = OMe; Table 1) having the melting point of 348–349 K, crystallizes as monohydrate (Gawroński *et al.*, 1997, and references therein). Although the crystal structure of this compound would be of interest, attempts to obtain suitable crystals for X-ray diffraction have been unsuccessful. We might anticipate, however, that this crystal structure will be governed by patterns similar to those found in (*R*,*R*)-tartaric acid (Okaya *et al.*, 1966) and HOH2 (Rychlewska *et al.*, 1999) with molecules arranged head-to-tail along the axis of length approximately 7 Å, and water molecules connecting the chains *via* OH···O*W*H···O═C hydrogen bonds. The other derivative belonging to the investigated series, for which the crystal structure is not yet known, is *R*,*R*-tartaric acid mono(*N*-methylamide) monomethyl ester (*X* = OMe, *Y* = NHMe, m.p. 414–418 K; Gawroński *et al.*, 1997). The sample does not fit into the proposed generalization, because its melting point is much higher than expected from the donor-to-acceptor ratio. The inclusion of solvent water molecules in the calculations changes favourably the donor-to-acceptor ratio. Another possibility is that HOM2 molecules adopt a basically different conformation in the crystal which eases the packing, as is the case for (*R*,*R*)-*N*,*N*,*N*′,*N*′-tetramethyltartramide (Gawroński *et al.*, 1989).

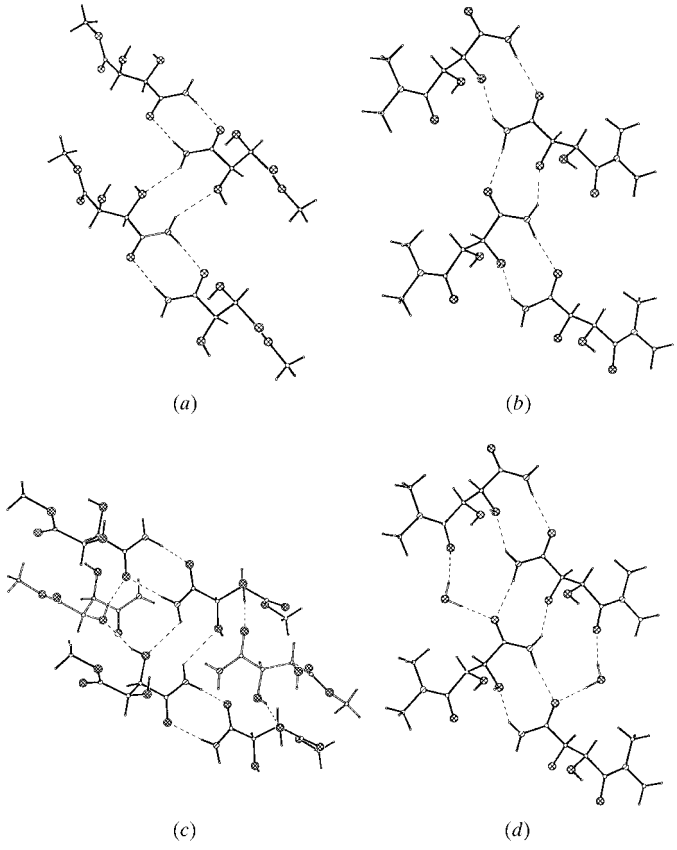

Figure 14
Similarities in packing in the crystal structures of (*a*) HOM1 and (*b*) HN13 described by the common pattern designator $R_4^4(16)$. (*c*) Further extension of this pattern in HOM1 by means of a second set of molecules which differ in conformation from their neighbours by a 180° rotation around one of the two Csp^3—Csp^2 bonds. (*d*) In HN13 where such changes of conformation are precluded, the molecules are further connected by hydrogen bonds *via* mediating water molecules.

4. Conclusions

(*R*,*R*)-Tartramides, being highly functionalized molecules, aggregate in such a way as to promote multiple point dimeric and trimeric interactions rather than single point interactions. Accordingly, they form many, consequently rather weak, hydrogen bonds in which carbonyl groups act as multiple acceptors, and amide H atoms (N—H_{trans} in particular) and hydroxyl H atoms act as multiple donors. Of the many types of hydrogen bonds described, those to the acid or amide carbonyl O atoms, from either a hydroxyl or amide substituent, seem to be the main driving force for the molecular association of primary tartramides. While the N—H···O(ester) hydrogen bonds are not observed at all, the O—H···O═C(ester) hydrogen bonds are significantly longer than the analogous bonds to amide or carboxyl carbonyls. The OH···OH hydrogen bonds always constitute part of the OH···OH···O═C chain or ring motif which is present in all but one of the crystal structures. Therefore, this hydrogen-bond arrangement, formed in many different ways, might be considered as universal in the investigated series. However, it seems to play a dominant role only in those derivatives which contain methylester or methylamide substituents. In these

compounds realisation of the OH···OH···O=C pattern requires either multimolecular asymmetric units or the presence of solvent water molecules.

Intramolecular hydrogen bonds [all described by an $S(5)$ pattern designator] join only proximal functional groups. This has an analogy in complexing properties of tartrates: the metal ions are most frequently embedded into a five-membered chelate ring.

Patterns dictated by amide groups would consist of a set of chains that run along the screw axis of an identity period of approximately 5–6 Å, and/or ring systems formed between like-to-like or like-to-unlike complementary groups such as α-hydroxyamide, α-hydroxyacid, α-hydroxyester, amide and hydroxyl functions. Originating from the parent tartaric acid are the $C(7)$ chain motifs that join molecules related by approximately 7 Å translation or ring patterns that join both ends of the β-hydroxycarbonyl units. Realisation of such patterns would often require the presence of solvent water molecules.

Analysis of packing of the two tartramic acids that form crystals at room temperature (HOH1, HOH2) suggests that in tartramic acid the packing is dictated by the presence of primary amides, while in *N*-methyltartramic acid it is governed by the carboxyl function. This seems to indicate a dramatic difference between the hydrogen-bond donating abilities of primary and secondary amides. The observed difference might result from steric constraints that restrict the number and geometry of hydrogen bonds formed by secondary amides.

The packing problems of methylated derivatives are overcome by crystallization with multi-molecular asymmetric units (esters) or water molecules (secondary and tertiary amides). The steric bulk of mono- and dimethylamide substituents combined with different conformational preferences of secondary and tertiary α-hydroxyamide groups might prevent crystallization of the *N*,*N*,*N*′-trimethylamide derivative, which is liquid at room temperature as is (*R*,*R*)-*N*,*N*-dimethyltartramic acid.

As a rule, symmetrically substituted (*R*,*R*)-tartaric acid esters and amides do not maintain their C_2 symmetry in crystals, although they crystallize in space groups possessing this symmetry element, *e.g.* $P4_12_12$ (HN12, Table 4). In such a case, the twofold rotation axis functions as a means of producing dimers from homochiral molecules. A similar role is played by multi-molecular asymmetric units.

Extended hydrogen-bond patterns, observed in the majority of the crystal structures described, influence the macroscopic behaviour of crystals; the values of their melting points decrease in order of the decreasing ratio of hydrogen-bond donors to acceptors.

The authors wish to thank Professor J. Gawroński for providing the samples for X-ray analysis and for his stimulating interest in this work.

References

Aakeröy, C. B. (1997). *Acta Cryst.* B**53**, 569–586.

Berkovitch-Yellin, Z., Ariel, S. & Leiserowitz, L. (1983). *J. Am. Chem. Soc.* **105**, 765–767.

Berkovitch-Yellin, Z. & Leiserowitz, L. (1982). *J. Am. Chem. Soc.* **104**, 4052–4064.

Bernstein, J., Davis, R. E., Shimoni, L. & Chang, N. L. (1995). *Angew. Chem. Int. Ed. Engl.* **34**, 1555–1573.

Bernstein, J., Etter, M. C. & Leiserowitz, L. (1994). *Structure Correlation*, edited by H. B. Bürgi and J. D. Dunitz, ch. 11, Vol. 2, pp. 431–507. Weinheim: VCH Publishers.

Bootsma, G. B. & Schoone, J. C. (1967). *Acta Cryst.* **22**, 522–532.

Brock, C. P. & Duncan, L. L. (1994). *Chem. Mater.* **6**, 1307–1312.

Brock, C. P. & Dunitz, J. D. (1994). *Chem. Mater.* **6**, 1118–1127.

Carlström, D. (1973). *Acta Cryst.* B**29**, 161–167.

Desiraju, G. R. (1989). *Crystal Engineering: The Design of Organic Solids.* Amsterdam: Elsevier.

Duesler, E. N., Mondragon, M. & Tapscott, R. E. (1984*a*). *Acta Cryst.* C**40**, 1286–1288.

Duesler, E. N., Mondragon M. & Tapscott, R.E. (1984*b*). *Acta Cryst.* C**40**, 1887–1890.

Etter, M. C. (1990). *Acc. Chem. Res.* **23**, 120–126.

Flippen, J. (1973). *Acta Cryst.* B**29**, 1881–1886.

Foster, S. J. & James, V. J. (1983). *Acta Cryst.* C**39**, 610–612.

Fun, H.-K. & Sivakumar, K. (1995). *Acta Cryst.* C**51**, 2085–2087.

Gałdecki, Z., Kowalski, A. & Uszyński, L. (1995). *DATAPROC Data Processing Program.* Version 9. Kuma Diffraction, Wrocław, Poland.

Gavezzotti, A. (1994). *Acc. Chem. Res.* **27**, 309–314.

Gawroński, J. & Gawrońska, K. (1999). *Tartaric and Malic Acids in Synthesis.* New York: John Wiley and Sons, Inc.

Gawroński, J., Gawrońska, K. & Rychlewska, U. (1989). *Tetrahedron Lett.* **30**, 6071–6074.

Gawroński, J., Gawrońska, K., Skowronek, P., Rychlewska, U., Warżajtis, B., Rychlewski, J., Hoffmann, M. & Szarecka, A. (1997). *Tetrahedron*, **53**, 6113–6144.

Hoffmann, M., Rychlewski, J. & Rychlewska, U. (1999). *J. Am. Chem. Soc.* **129**, 1912–1921.

Hommeltoft, S. I., Cameron, A. D., Shackleton, T. A., Fraser, M. E., Fortier, S. & Baird, M. C. (1986). *Organometallics*, **5**, 1380–1388.

Jeffrey, G. A. (1994). *J. Mol. Struct.* **322**, 21–25.

Jeffrey, G. A. & Saenger, W. (1991). *Hydrogen Bonding in Biological Structures.* Berlin, Heidelberg: Springer-Verlag.

Kennard, O. & Allen, F. H. (1993). *Chem. Des. Autom. News*, **8**, 1, 31–37.

Kivikoski, J., Vepsäläinen, J., Suontamo, R., Pohjala, E. & Laatikainen, R. (1993). *Tetrahedron Asym.* **4**, 709–722.

Kroon, J. (1982). *Molecular Structure and Biological Activity*, edited by J. F. Griffin and W. L. Luax, pp. 151–163. Buffalo: Elsevier Biomedical.

Kuma Diffraction (1991). *KM*-4 *User's Guide*, Version 3.2. Kuma Diffraction, Wrocław, Poland.

Larsen, S. & Marthi, K. (1994). *Acta Cryst.* B**50**, 373–381.

Leiserowitz, L. (1976). *Acta Cryst.* B**32**, 775–802.

Leiserowitz, L. & Hagler, A. T. (1983). *Proc. R. Soc. London Ser. A*, **388**, 133–175.

Leiserowitz, L. & Schmidt, G. M. J. (1969). *J. Chem. Soc. A*, pp. 2372–2382.

Leiserowitz, L. & Tuval, M. (1978). *Acta Cryst.* B**34**, 1230–1247.

Marthi, K., Larsen, S., Ács, M., Bálint, J. & Fogassy, E. (1995). *Acta Chem. Scand.* **49**, 20–27.

Okaya, Y., Stemple, N. R. & Kay, M. I. (1966). *Acta Cryst.* **21**, 237–243.

Pedersen, S. F., Dewan, J. C., Eckman, R. R. & Sharpless, K. B. (1987). *J. Am. Chem. Soc.* **109**, 1279–1282.

Polavarapu, P. L., Ewing, C. S. & Chandramouly, T. (1987). *J. Am. Chem. Soc.* **109**, 7382–7386.

Rychlewska, U. (1992). *Acta Cryst.* C**48**, 965–969.

Rychlewska, U., Szarecka, A., Rychlewski, J. & Motała, R. (1999). *Acta Cryst.* B**55**, 617–625.

Rychlewska, U., Warżajtis, B., Hoffmann, M. & Rychlewski, J. (1997). *Molecules*, **2**, 106–113.
Rychlewski, J. & Szarecka, A. (2000). Unpublished results.
Schouten, A., Kanters, J. A. & van Krienen, J. (1994). *J. Mol. Struct.* **323**, 165–168.
Sheldrick, G. M. (1990). *Acta Cryst.* A**46**, 467–473.
Sheldrick, G. M. (1993). *SHELXL*93. University of Göttingen, Germany.
Siemens (1989). *Stereochemical Workstation Operation Manual.* Release 3.4. Siemens Analytical X-ray Instruments, Inc., Madison, Wisconsin, USA.
Szarecka, A., Hoffmann, M., Rychlewski, J. & Rychlewska, U. (1996). *J. Mol. Struct.* **374**, 363–372.
Szarecka, A., Rychlewska, U. & Rychlewski, J. (1999). *J. Mol. Struct.* **474**, 25–42.
Szarecka, A., Rychlewski, J. & Rychlewska, U. (2000). *Prog. Theoret. Chem. Phys.* **II**, 355–366.
Szczepańska, B. & Rychlewska, U. (1994). *Correlations, Transformations and Interactions in Organic Chemistry*, edited by D. W. Jones and A. Katrusiak, pp. 233–244. Oxford University Press.
Toda, F., Tanaka, K., Nassimbeni, L. & Niven, M. (1988). *Chem. Lett.* pp. 1371–1374.
Wash, P. L., Maverick, E., Chiefari, J. & Lightner, D. A. (1997). *J. Am. Chem. Soc.* **119**, 3802–3806.
Weinstein, S. & Leiserowitz, L. (1980). *Acta Cryst.* B**36**, 1406–1418.
Yamashita, M., Okuyama, K., Kawasaki, I. & Ohta, S. (1996). *Tetrahedron Lett.* **37**, 7755–7756.